Title

Effect of Thermal Fluctuations on the Radiative Rate in Core/Shell Quantum Dots

Journal

Nano Letters, 17(3)

ISSN

1530-6984

Authors

Balan, Arunima D

Eshet, Hagai

Olshansky, Jacob H

et al.

Publication Date

2017-03-08

DOI

10.1021/acs.nanolett.6b04816

Peer reviewed

NANO LETTERS

Letter

pubs.acs.org/NanoLett

Effect of Thermal Fluctuations on the Radiative Rate in Core/Shell Quantum Dots

Arunima D. Balan,[†,‡,§] Hagai Eshet,[∥,⊥] Jacob H. Olshansky,[†,‡,§] Youjin V. Lee,[†] Eran Rabani,*[,†,‡,⊥] and A. Paul Alivisatos*[,†,#,‡,§]

[†]Department of Chemistry, University of California, Berkeley, Berkeley, California 94720, United States

[‡]Materials Sciences Division, Lawrence Berkeley National Laboratory, Berkeley, California 94720, United States

[§]Kavli Energy NanoScience Institute, Berkeley, California 94720, United States

[∥]School of Chemistry, The Sackler Faculty of Exact Sciences and [⊥]The Raymond and Beverly Sackler Center for Computational Molecular and Materials Science, Tel Aviv University, Tel Aviv 69978, Israel

[#]Department of Materials Science and Engineering, University of California, Berkeley, California 94720, United States

S *Supporting Information*

ABSTRACT: The effect of lattice fluctuations and electronic excitations on the radiative rate is demonstrated in CdSe/CdS core/shell spherical quantum dots (QDs). Using a combination of time-resolved photoluminescence spectroscopy and atomistic simulations, we show that lattice fluctuations can change the radiative rate over the temperature range from 78 to 300 K. We posit that the presence of the core/shell interface plays a significant role in dictating this behavior. We show that the other major factor that underpins the change in radiative rate with temperature is the presence of higher energy states corresponding to electron excitation into the shell. These effects should be present in other core/shell samples and should also affect other excited state rates, such as the rate of Auger recombination or the rate of charge transfer.

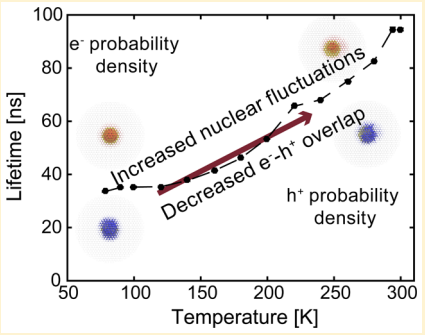

KEYWORDS: *Core/shell quantum dots, temperature-dependent lifetime, exciton dynamics, electronic structure*

Quantum dots (QDs) have received significant attention for their bright, narrow, and tunable emissions.[1−3] These properties, along with their increased photostability when compared to molecular dyes, make them promising candidates for a number of applications, including as emitters for LEDs and in displays,[4,5] as photosensitizers for QD-based solar cells,[6−9] and as fluorescent tags for bioimaging.[10,11] The relationship between the radiative, nonradiative, and charge transfer rates is one factor that determines the efficiency of such applications, with applications requiring bright QD emission reliant on maximization of the radiative rate, while minimizing undesirable nonradiative processes.

In applications that aim to maximize radiative recombination, an epitaxially grown shell is often used, but adds another degree of complexity to the system and modulates the excited state rates. For example, the addition of a Type-I shell confines both carriers to the core of the QD resulting in decreased surface trapping and therefore often a slower nonradiative rate.[1,11] However, the presence of the core/shell interface can result in charge localization near the interface and faster nonradiative Auger recombination.[12] The thickness of the shell and band offset between core and shell will determine the rate of charge tunneling to the surface[13,14] as well as directly modulate the radiative rate by changing the overlap integral. Significant work has been done to elucidate the effects of epitaxial shell growth on recombination rate, including effects of band offsets, interfacial alloying, and lattice strain.[15−17] For the most part, these studies treat both core and shell statically in order to determine excited state rates. A statistical treatment of QD excited state rates is of interest, because fluctuations can play a larger role in determining excited state properties in QDs than in bulk systems due to the smaller size of the QD.

We seek to elucidate the effect of fluctuations on the radiative rate in core/shell QDs. In bulk semiconductors, the sub-band gap absorption feature resultant from nuclear fluctuations and disorder, known as the Urbach tail, has been extensively studied.[18,19] In the bulk, fluctuations in nuclear positions average to create a density of states just below the bandgap. Because of the small electron−hole interaction in the bulk, this feature can often be described without considering electron−hole interactions; however in nanoscale systems the electron−hole interaction can be much stronger and therefore nuclear fluctuations could influence the radiative lifetime (which is dependent upon the electron−hole interaction). One way to determine the impact of nuclear fluctuations is to study the temperature-dependent optical properties, as nuclear motion is

Received: November 17, 2016
Revised: February 8, 2017
Published: February 10, 2017

DOI: 10.1021/acs.nanolett.6b04816
Nano Lett. XXXX, XXX, XXX−XXX

highly temperature-dependent. Previous studies on the temperature-dependent lifetime of QDs have been useful in elucidating QD properties. These techniques have been used extensively in order to evaluate the energetic splitting and radiative rates of the "dark" and "bright" excitonic states.[20−25] Similarly, the effects of lattice fluctuations on radiative recombination can be seen at temperatures between 5 and 50 K due to the presence of an optical phonon bottleneck, resulting in slower carrier relaxation to the band edge.[26−28]

Further understanding the effect of lattice fluctuations on QD properties requires input from theory; this has proven challenging due to the need to model systems involving thousands of nuclei and electrons. So far, the effects of lattice fluctuations on the electronic properties of nanocrystal QDs have been limited to fairly small systems.[29] The presence of surface and interfacial defects can also result in carrier trapping that requires complex modeling, but it is often difficult to precisely define the nature of such defects.[15,30,31] An additional complication with operating in intermediate temperature regimes (above 77 K) is that time-resolved photoluminescence convolutes the radiative and nonradiative rates. For particles with low photoluminescence quantum yield (PLQY), often it is the nonradiative rate that determines the change in the excited state lifetime, τ, over this temperature regime, because $\tau^{-1} = k_{nr} + k_r$ where k_{nr} is the nonradiative rate and k_r is the radiative rate.[32]

We chose CdSe/CdS as a model core/shell system due to its prevalence in the literature and the ability to make high PLQY particles of varying core and shell size.[1] In these heterostructures, the hole is localized to the CdSe core, which both improves the PLQY and increases the photostability of the core/shell heterostructure.[1] The electron, however is weakly confined to the core due to a small conduction band offset and a Coulomb attraction to the confined hole, resulting in a radiative rate dependent on both core and shell size.[33] Previous studies have shown that in CdSe/CdS QDs of both spherical and dot-in-rod geometries, the lifetime increases with temperature and posited that a changing, temperature-dependent conduction band offset could describe this effect.[34,35] However, models suggest that the change in band offset over the studied temperature range (~20 meV using bulk parameters) is insufficient to describe the change in radiative rate with temperature given a conduction band offset of 300 meV.[36] Therefore, questions still remain on the mechanism of this change in radiative rate with temperature. Furthermore, the lack of computational support for the experimental measurements limits the conclusions that can be drawn, as a number of factors could influence the observed behavior.

We use spherical CdSe/CdS core/shell QDs to study the effect of both nuclear fluctuations and the effect of higher-lying electronic excited states on the radiative rate using a combination of temperature-dependent transient photoluminescence experiments and atomistic pseudopotential calculations. To determine the impact of nuclear fluctuations, we ran molecular dynamics simulations. For a set number of these configurations, we take nuclear snapshots and then perform a full electronic structure calculation. By averaging over these snapshots, we can simulate the impact of nuclear fluctuations on the electronic properties.

Wurtzite CdSe/CdS core/shell were synthesized according to Chen at al.[1] Two different sizes of CdSe cores were prepared with three different shell thicknesses per core sample, as shown in Table 1. Calculations are done on particles with sizes

Table 1. Sizes and PLQY of CdSe/CdS QD synthesized

core diameter [nm]	total diameter (error) [nm]	PLQY (error) at RT
3.4	7.5 (0.8)	0.76 (0.02)
3.4	9.7 (0.7)	0.84 (0.03)
3.4	12.5 (1.0)	0.89 (0.05)
4.9	9.7 (0.9)	0.52 (0.02)
4.9	10.9 (1.8)	0.60 (0.04)
4.9	13.1 (2.2)	0.58 (0.04)

comparable to four of the six synthesized samples, which are particles with 3 and 5 nm diameter cores and 9 and 12 nm total diameters. Representative experimental photoluminescence data across the temperature range studied are shown in Figure 1. The synthesized QDs are spherical with a narrow size distribution, as seen via transmission electron microscopy (TEM) and have high PLQY; see Supporting Information for further details. We note that the emission spectra, particularly at low temperature, appear asymmetric. This is likely due to reduced homogeneous (and symmetric) broadening at lower temperature. Therefore, inhomogeneous broadening in the sizing distribution becomes more apparent. Processed emission data fit the empirical Varshni relation, $E_G(T) = E_G(0) - \frac{\alpha T^2}{T+\beta}$, where α is a measure of electron−phonon coupling and β is related to the Debye temperature with parameters $E_G(0) \sim 2.08$ [eV], $\alpha \sim 4 \times 10^{-4}\left[\frac{eV}{K}\right]$, and $\beta \sim 110$ [K], comparable to those of bulk CdSe, except for the 0 K band gap that is larger due to the quantum confinement of the QD. The full width at half-maximum increases with temperature, as is expected given the effects of exciton−phonon coupling. Both features indicate that the emission originates from the CdSe core of the QD, consistent with previous measurements.[34,35]

Notably, the lifetime increases with increasing temperature for the CdSe/CdS samples, as shown in Figure 1c,d. Because these QDs have a high PLQY, we note that this change in lifetime with temperature is primarily due to a change in the radiative rate in the material. Temperature-dependent PLQY of the 3.4 nm core diameter samples, shown in the Supporting Information, confirms this assumption. For all samples studied, the PLQY is higher at low temperatures (approximately a 10−20% change), indicating a decreased nonradiative rate at lower temperatures. This suggests that although there can be significant nonradiative rates present, the change over this temperature regime does not explain the increase in excited state lifetime with temperature as an increased nonradiative recombination rate at higher temperatures would only serve to enhance this observation. We also note that the rate of exciton thermalization, observed in CdSe/CdS dot-in-rods to be <1 ps for the hole, is much faster than the radiative rate.[37] Therefore, we can safely assume that the exciton is in thermal equilibrium. Within this assumption, the presence of higher order electronic states would not affect the observed exponential decay of the time-resolved photoluminescence spectra. The presence of monoexponential behavior at early times is also indicative of an exciton that has already thermalized to the band edge, shown in Figure 1c. For example, at 78 K the radiative decay appears monoexponential over 3 orders of magnitude. There is increasing nonmonoexponential character for higher temperature samples but they still remain monoexponential over much of the first two decades. Owing to inconsistencies in weighting in biexponential fit parameters, we fit all decays to a monoexponential over the first decade and a half; we note

DOI: 10.1021/acs.nanolett.6b04816
Nano Lett. XXXX, XXX, XXX−XXX

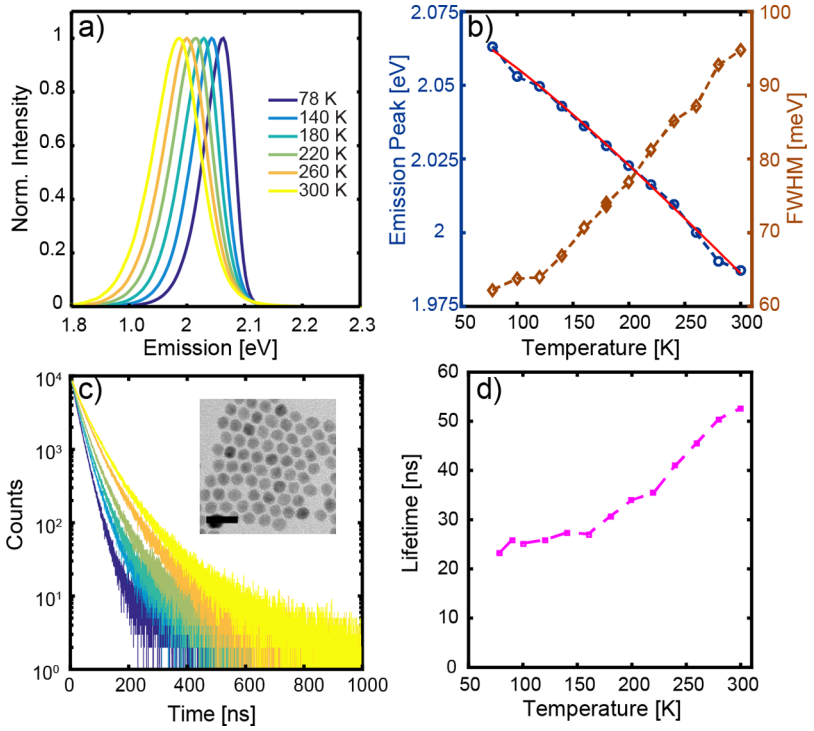

Figure 1. Sample data using the 3.4 nm core, 9.7 nm total diameter CdSe/CdS sample. (a) Normalized temperature-dependent emission spectra and (b) temperature-dependence of the PL peak energy and peak width. The red line indicates the Varshni fit for optical band gap versus temperature for the sample. (c) Time-resolved PL spectra taken at the same temperatures as panel a. The inset shows a sample TEM of the QD with a 25 nm scale bar. (d) Temperature-dependent lifetime fits.

that although this might introduce a small systematic error into our fits, the relationship between the fits will still hold.

The energy scales in the system determine which fluctuations are relevant in dictating radiative behavior over the temperature range studied. For quantum confined systems, an understanding of the relevant energy scales is complicated by the additional strong electron−hole interactions. The energy scales for CdSe/CdS QD excitations are presented in Figure 2. The conduction and valence band offsets have previously been determined.[38] Although there is a 300 meV band offset in the conduction band, the electron's kinetic energy is of the same scale, so the electron is not completely confined to the core

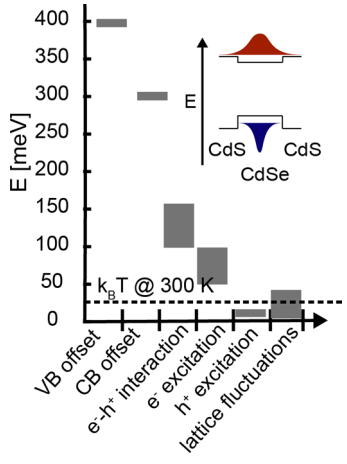

Figure 2. Relevant energy scales for CdSe/CdS QD excitations. The inset (not to scale) shows a schematic of the CdSe/CdS band alignment and electron (red) and hole (blue) probability densities.

(neglecting electron−hole interactions). The hole kinetic energy is less than the electron kinetic energy due to its larger effective mass; this coupled with the large valence band offset effectively confines the hole to the core. We calculate the electron−hole interaction to be on the order of ∼150 meV as shown in Figure 3c,d, resulting in further confinement of the electron to the core. In addition to understanding the energy scales of the ground state exciton, it is also necessary to note the energy scales of higher excitations. Hole excitation takes <10 meV of energy, while electron excitation is strongly dependent on the core and shell sizes of the CdSe/CdS, ranging from 50 to 120 meV. Further information about the energies relevant to exciton excitation can be viewed in the Supporting Information.

Lattice fluctuations can be quantified as phonon modes and occupy a large energy range, but as a lower bound confined acoustic phonons have an energy scale on the order of 1 meV.[39] Previous work has used temperature to probe the dependence of coupling to acoustic phonons in CdSe QDs and has indicated that the deformation potential is larger in smaller CdSe cores.[40] We would expect optical phonons to have excitations on the order of tens of millielectronvolts, and this would be the upper bound of the energy scales for lattice excitations. Therefore, at room temperature (∼300 K) the main thermally accessible excitations involve those accessed by hole excitation and lattice vibrations. In addition, electron excitation into the shell is a possibility. Therefore, the root cause of the change in radiative lifetime with temperature must be influenced by these factors. For this reason, we confine further discussion to primarily lattice fluctuations with some discussion of contribution from higher electronic excitations.

Another effect for which fluctuations are important is the temperature dependence of the CdSe emission peak energy,

DOI: 10.1021/acs.nanolett.6b04816
Nano Lett. XXXX, XXX, XXX−XXX

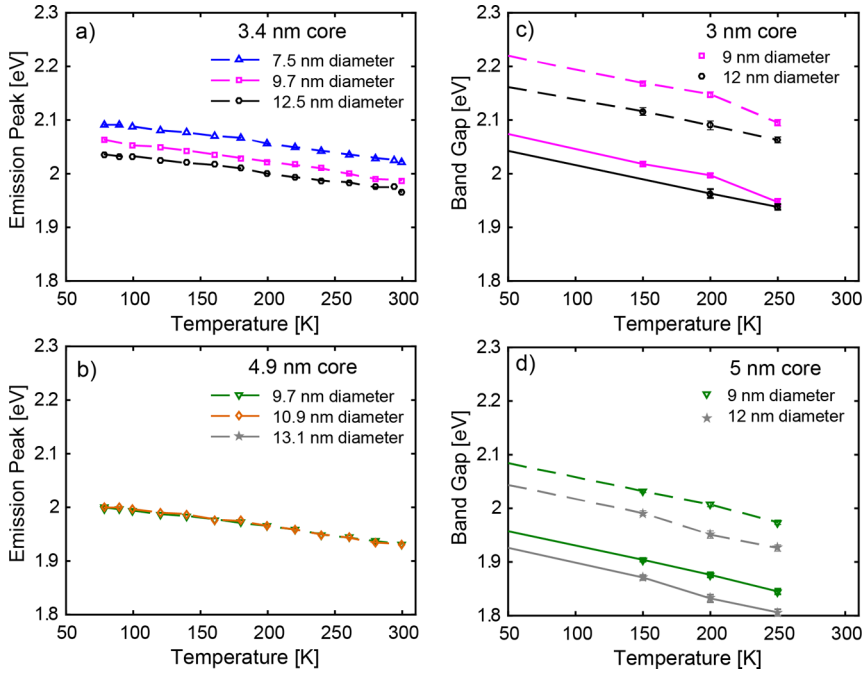

Figure 3. (a,b) Dependence of emission peak on temperature for a given CdSe core diameter, and three total diameters. (c,d) Computed dependence of the energy gap on temperature for simulated CdSe/CdS QDs. The dashed lines represent the fundamental gap and the solid lines represent the exciton gap. Computational error bars arise from averaging over a number of nuclear configurations.

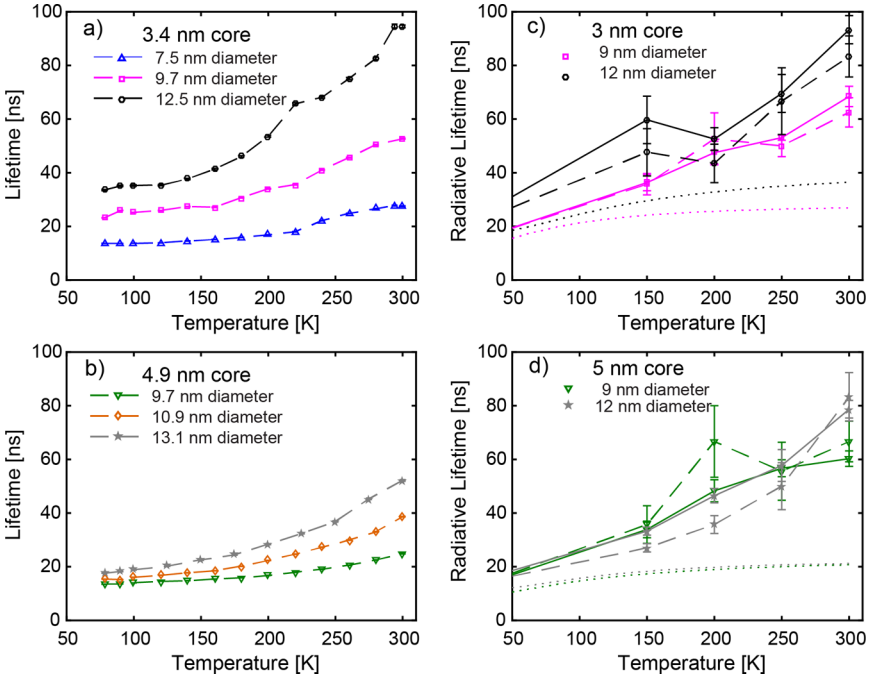

Figure 4. Experimental temperature dependence of the excited state lifetime for CdSe/CdS QDs. (c,d) Computed temperature dependence of the radiative lifetime for simulated CdSe/CdS QDs. The effects of thermal excitation (dotted line), thermal fluctuations (dashed line), and both thermal excitation and fluctuations (solid) line are shown for all particle sizes studied. Computational error bars arise from averaging over a number of nuclear configurations.

which shifts by ~80 meV between 78 and 300 K. Using bulk parameters, the change in band gap due to thermal expansion of the lattice is only 8 meV over the same temperature range; the other 90% of the observed change in band gap with temperature is due to coupling between electronic states and lattice fluctuations, consistent with the empirical parameters present in the Varshni fit. For this reason, before simulating the radiative lifetime at different temperatures, it is possible to assess the accuracy of our atomistic model by comparing the calculated and measured change in the band gap with temperature, which we have done at 0, 150, 200, and 250 K. Shown in Figure 3a,b are the experimentally observed change in emission peak with temperature. Figure 3c,d shows the theoretical calculations of the CdSe/CdS optical band gap for

DOI: 10.1021/acs.nanolett.6b04816
Nano Lett. XXXX, XXX, XXX−XXX

similar core and shell sizes. The resulting calculations, which match well to the experimental data, predict a change in the emission peak of approximately 100 meV; the change in the band gap appears to be approximately 80 meV for the experimental data over the same temperature range. Similarly, the difference between theory and experiment in the absolute values of the band gap of the material is less than 20 meV for the small core samples.

For the large core samples, the deviation between computation and experiment is slightly larger on the order of 40−50 meV. The experimental large core samples show almost no dependence of the emission peak on the shell thickness. This trend is reasonable, as a larger core would result in both electron and hole being more confined to the core and being less sensitive to the shell thickness. However, the comparison between theory and experiment does not perfectly capture this behavior, suggesting potentially a scaling inconsistency between the theory and experiment. Indeed, for larger shell sizes the theory does show saturation of the band gap with shell thickness, as shown in the Supporting Information. Such an inconsistency is possible given the approximations required for the computations. The use of a semiempirical pseudopotential model for the electronic structures, the static screening approximation for the Bethe−Salpeter calculations, and a force-field approximation to simulate nuclear configurations could all introduce small errors. Furthermore, the experiments measure the fluorescence peak of the QDs whereas we compute the band gap directly, introducing the possibility of differences between theory and experiment. The small differences between the theoretical and experimental sizes for the core/shell QDs, as well as the presence of a size distribution in the experimental data, could also contribute to the error.

However, we emphasize that despite these discrepancies we have close correspondence between theory and experiment; agreement to tens of millielectronvolts between electronic structure computations and the experiment is quite successful. The importance of including the electron−hole interactions when calculating the energy gap is also highlighted in Figure 3; this interaction reduces the energy gap by ∼150 meV for the samples considered, consistent with previous measurements.[38] The close correspondence between experiment and theory indicates that the theoretical simulations are accurate enough to proceed with more complex calculations of the radiative lifetime at different temperatures.

Figure 4a,b shows the experimental dependence of the CdSe/CdS excited state lifetime on temperature. We see that for all samples there is an increase of the lifetime with increasing temperature. This feature is most prominent for the samples with thicker shells. Additionally, the 3.4 nm core sample shows the greatest change in excited state lifetime over the temperature regime studied. Previous studies have ascribed the increase in lifetime with increasing temperature in CdSe/CdS QDs to increased electron delocalization into the shell.[34,35] As the major changes within the lattice over this temperature regime involve nuclear fluctuations, we need to understand how these nuclear fluctuations change both electron and hole probability densities, which our simulations will achieve. Furthermore, as noted previously (see Supporting Information for further details), particularly for the large shell, small core particles, there are low-lying electronic states that could become populated at increased temperature. Thermal population of these states could change the radiative lifetime for CdSe/CdS QDs. To deconvolute these two factors requires the input of theory. Figure 4c,d shows the computed change in radiative lifetime, $\tau_r = k_r^{-1}$, due to thermal electronic excitation versus thermal fluctuations of the nuclei. We note spin−orbit coupling is not included in the calculation, so there may be a systematic error. However, we expect the relative change in radiative lifetime to be comparable.

The effect of thermal population of higher energy excitonic states on the radiative lifetime is shown by the dotted lines of Figure 4c,d. The calculation also incorporates the expected change in the radiative lifetime due to the frequency-dependence of spontaneous emission (approximately a 15% increase in the radiative lifetime) resulting from the change in the exciton energy. It is clear that thermal population is insufficient to describe the change in radiative lifetime and only accounts for 20−30% of the observed experimental change. The effect of thermal population does, however, match the observed trends of smaller cores and larger shells having larger changes in lifetime. These trends are further explained in the Supporting Information, where we show that the thermal energy could generate two types of excited electron−hole states. The more common and lower energy involves primarily hole levels and is confined to the core. These excitations are thermally accessible to all systems studied. The other less common and higher energy excitation involves mainly electron levels, is delocalized in the shell (which therefore would impact the radiative lifetime), and is more likely to occur for small cores and large shells. Thus, samples with small cores and large shells exhibit the greatest increase in radiative lifetime with temperature. This behavior explains the computed and measured trends with system size; however, as previously described, thermal population by itself is not sufficient to quantify the experimental behavior.

In Figure 4c,d, we also plot the computed radiative lifetime as a function of temperature when only lattice fluctuations are included (dashed lines). This is achieved by simulating a number of potential nuclear configurations and calculating the radiative lifetime for the ground excitonic state for each nuclear configuration. We then average these values to compute the radiative lifetime as a function of temperature. The magnitude of the observed change in lifetime with temperature due to nuclear fluctuations is comparable to the experimental results, but it is difficult to determine how the change in lifetime with temperature caused by nuclear fluctuations depends on the core and shell dimensions of the QDs. The role of the shell thickness is more evident for the 3 nm diameter core, where there is a clear difference in the room-temperature radiative lifetimes due solely to nuclear fluctuations of the 9 and 12 nm total diameter particles (Figure 4c); this matches well with the observed experimental data (Figure 4a). For the 5 nm core size, the difference in the calculated room-temperature radiative lifetimes for the two total diameters is within the statistical error of the calculations (Figure 4d). The reduced impact of shell thickness for the 5 nm cores suggests that the larger core reduces the impact of fluctuations, likely because there is much less electron density near the core/shell interface. We note that because of the small number of configurations used to average the results (between 10 and 20), the results are noisy and show a nonmonotonic behavior in the dependence of the radiative lifetime with temperature. The latter can result from a "locking" effect, where certain configurations lead to hole trap states near the surface that also lock the electron on the surface due to strong electron-hole interactions. We expect that the inclusion

DOI: 10.1021/acs.nanolett.6b04816
Nano Lett. XXXX, XXX, XXX−XXX

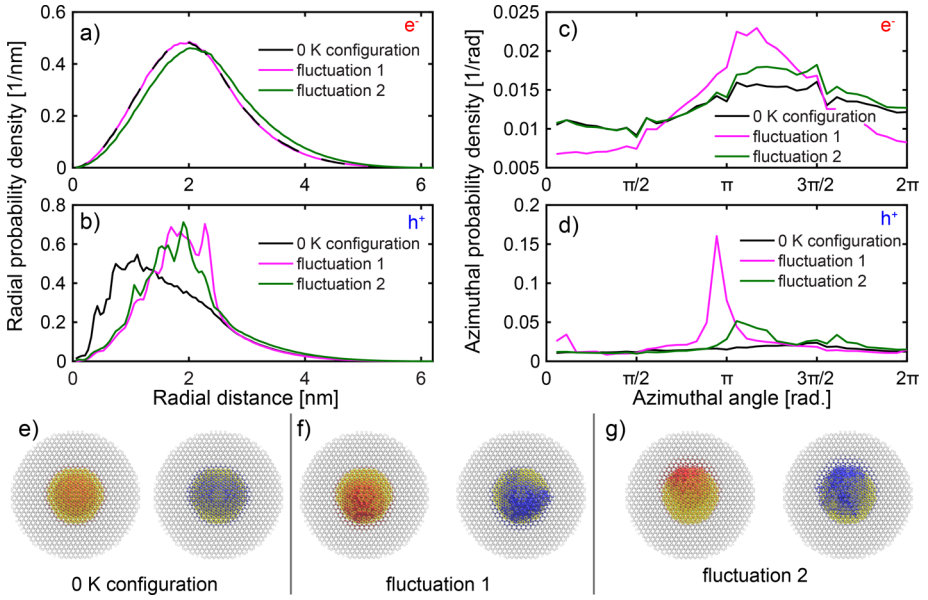

Figure 5. Radial probability density for the electron (a) and hole (b) for the 5 nm core diameter, 12 nm total diameter particle, shown for the 0 K configuration and two sample fluctuations computed at 250 K. The azimuthal probability density computed over a shell of thickness 0.8 nm at the core/shell interface for the same particle and fluctuations is shown for the electron (c) and hole (d). (e–g) The probability densities for electron (left, red) and hole (right, blue) for the same three sampled configurations. The yellow region corresponds to the CdSe core.

of a greater number of nuclear configurations would reduce this feature.

The effect of both lattice fluctuations and thermal population of excited states is shown by the solid lines in Figure 4c,d, and most accurately corresponds to the observed experimental data. We compute this by additionally averaging over thermally accessible excitonic states for each nuclear configuration. By including both the effects of thermal population of excited states and thermal fluctuations of the lattice, we recover the observed difference in the temperature dependence for different shell sizes for the large core particles. With the incorporation of both the effects of thermal excitations and nuclear fluctuations, the nonmonotonic behavior discussed above is not as prominent, and more closely matches the experimental data. This suggests that although some local, transient trapping of the exciton could occur, these events are averaged out. The calculated results and the experimental results show the greatest deviations at temperatures near room temperature; this is the most evident for the comparison for the large core samples. This is partially a result of the lower PLQY of the experimental 4.9 nm core diameter samples, which results in a shorter lifetime due to nonradiative quenching. Small differences between computational and experimental results are unsurprising; the experiment averages over a large number of potential lattice configurations, whereas we sample only one QD structure and simply allow the nuclear positions to fluctuate computationally. There are other sources of error for this overestimation of the radiative lifetime; particularly at high temperatures, the discrepancy could be due to differences between the interfacial structure for the synthesized and modeled particles. For example, some alloying at the CdSe/CdS interface occurs during shell growth. Similarly, the facets presented by the core particles are variable and not well-defined, introducing a source of error in the comparison of the experiment and the calculations.

To gain a better understanding of the impact of lattice fluctuations on the radiative lifetimes, we plot in Figure 5 the probability densities for the hole and the electron at 0 K and for two sample configurations at 250 K, for the 5 nm core and 12 nm total diameter QD. Sample fluctuations for the other QD sizes are included in the Supporting Information and show similar features. Radial probability densities are shown in Figure 5 for both the electron (Figure 5a) and hole (Figure 5b). There are small but noticeable differences between the 0 K configuration and the two sample fluctuations for both electron and hole densities. We see delocalization of the electron into the shell in one sample fluctuation (magenta line) but less so in the other sample (green line) for which the radial electron density is nearly identical to the 0 K result. On the other hand, the hole localizes toward the interface between the core and shell in both sample fluctuations. Additional support for this is depicted in Figure 5c,d, where the angular distribution (over the azimuthal angle) averaged over a thin shell around the interface is shown. For the 0 K configuration, we see a negligible degree of angular asymmetry for the electron (Figure 5c) and hole (Figure 5d). However, the sample fluctuations show significant angular localization of the hole in both cases. The electron evidences a smaller increase in angular asymmetry due to the sample fluctuations as well and is correlated with the behavior of the hole.

When we visualize the electron and hole probability density maps, as shown in Figure 5e–g, we see that for the 0 K configuration (Figure 5e), both electron and hole probability densities are symmetric and primarily localized in the core. As we allow the nuclear positions to fluctuate (Figure 5f–g), both electron and hole probability densities exhibit increased asymmetry, and in the two fluctuations pictured result in localization of the hole near the core/shell interface, supporting the conclusions drawn from Figure 5a–d. In addition, it is evident that the electron–hole interaction is significant, as both electron and hole tend to move together with the electron more able in certain cases to delocalize into the shell. These results clearly suggest that the overlap between the electron and the hole is reduced when nuclear fluctuations are included

DOI: 10.1021/acs.nanolett.6b04816
Nano Lett. XXXX, XXX, XXX–XXX

because the degree of localization induced by lattice fluctuations is different for the electron and the hole.

The results presented highlight the importance of thermal fluctuations in determining excited state rates in QDs. In bulk materials, fluctuations in lattice positions have been shown to change the sub-band gap absorption;[18,19] in QDs, due to the strong electron−hole interaction these same fluctuations can change the radiative rate by a factor of 3 between 78 and 300 K. We demonstrate that inclusion of fluctuations at the atomic level is necessary in order to describe the temperature dependence of the radiative lifetime for QDs. Previous work has attempted to elucidate the source of the temperature dependence of the radiative lifetimes in nanostructured QDs[23,34] and quantum wells,[41,42] but it is difficult to demonstrate without a detailed theoretical model, which we have presented. We note that a small change in band offset, as postulated previously,[34,35] could contribute partially to the observed effect, but as shown by the probability densities of Figure 5e−g, hole motion is also relevant as is thermal population of excited states, neither of which were captured previously. We show that the presence of these nuclear fluctuations results in an electron−hole overlap that is highly dependent on both the core and shell dimensions. This indicates that temperature could have a significant effect on other rates for which the electron wave function is important, including charge transfer rates or Auger recombination. The magnitude of the impact of temperature on excited state rates is likely highly dependent on core and shell materials. Additional features that would likely tune the magnitude of the observed effects involve the degree of alloying and precise structure of the interface and provide opportunity for further investigations.

Experimental Methods. QDs were synthesized according to previous procedures.[1,13] Further information can be found in the Supporting Information. Room-temperature optical characterization was performed in hexanes, and PLQY was determined using a Rhodamine 6G reference or an integrating sphere technique.[43] Temperature-dependent photoluminescence measurements were taken using a time-correlated single photon counting apparatus consisting of a Picoquant Fluotime 300 spectrometer, a PMA 175 detector, and a LDH-P-C-405 diode laser with a 407 nm excitation wavelength (50 ps pulse width) and repetition rates varying between 500 kHz and 10 MHz. We note that the average number of excitons per pulse is $\ll 1$, so we do not consider multiexciton events. The temperature was tuned controllably via a Lakeshore 330 temperature control. Samples were typically prepared by dissolving a small amount of QDs in 2,2,4,4,6,8,8-heptamethylnonane or 3-methylpentane, optical glass forming solvents, and were loaded into a sample cell consisting of two sapphire windows and an inert spacer; then they were placed on a sample holder within a Janis ST-100 continuous flow optical cryostat.

Computational Methods. We constructed faceted core/shell CdSe/CdS nanocrystals with a spherical CdSe core placed at the center. The configurations used for the electronic structure calculations were equilibrated with molecular dynamics runs of 100 ps and temperatures varying between 150 to 300 K. For these runs, interactions between atoms were described by modification of the covalent Tersoff-type potential developed by Benkabou et al.[44] (See Supporting Information for a detailed description of simulation methods.)

The electronic structure calculations of the core/shell QDs were performed within the local version of the semiempirical pseudopotential model[45−47] where the local screened pseudopotentials were fitted to reproduce the experimental bulk band structure, band gaps, effective masses, and so forth.[33,48] The filter-diagonalization technique[49] was then employed to generate nearly 40 single particle filtered states near the conduction and valence band edges. These states were then used to solve the Bethe−Salpeter equation within the static screening approximation. In our calculation, we used 10 hole states and 20 electron states and verified that including more states does not affect the properties calculated.

■ ASSOCIATED CONTENT

Supporting Information

The Supporting Information is available free of charge on the ACS Publications website at DOI: 10.1021/acs.nanolett.6b04816.

Further details about the synthesis and sizing of QDs; additional spectroscopic data including room-temperature absorption, spectra and fits for temperature-dependent lifetime data, and temperature-dependent PLQY; additional computational methods; additional computational data and analysis of the band gap, temperature-dependent exciton structure, and electron and hole probability densities; additional instrumentation (PDF)

■ AUTHOR INFORMATION

Corresponding Authors

*E-mail: eran.rabani@berkeley.edu.
*E-mail: alivis@berkeley.edu.

ORCID

Arunima D. Balan: 0000-0002-9216-7806
Jacob H. Olshansky: 0000-0003-3658-1487
A. Paul Alivisatos: 0000-0001-6895-9048

Notes

The authors declare no competing financial interest.

■ ACKNOWLEDGMENTS

This work is supported by the Physical Chemistry of Inorganic Nanostructures Program, KC3103, Office of Basic Energy Sciences of the United States Department of Energy under Contract DE-AC02-05CH11231 and by the Laboratory Directed Research and Development Program of Lawrence Berkeley National Laboratory under U.S. Department of Energy Contract No. DE-AC02-05CH11231. A.D.B. and J.H.O acknowledge the National Science Foundation Graduate Research Fellowship under Grant DGE 1106400. A.D.B. acknowledges a Berkeley Graduate Fellowship. The authors acknowledge Dr. Son Nguyen and Dr. Jianbo Gao for assistance with the optical cryostat and Dr. Noah Bronstein for helpful discussions.

■ REFERENCES

(1) Chen, O.; Zhao, J.; Chauhan, V. P.; Cui, J.; Wong, C.; Harris, D. K.; Wei, H.; H-S, H.; Fukumura, D.; K, J. R.; Bawendi, M. G. *Nat. Mater.* **2013**, *12*, 445−451.
(2) Dabbousi, B. O.; Rodriguez, J.; Mikulec, F. V.; Heine, J. R.; Mattoussi, H.; Ober, R.; Jensen, K. F.; Bawendi, M. G. *J. Phys. Chem. B* **1997**, *101*, 9463−9475.
(3) Peng, Z. A.; Peng, X. *J. Am. Chem. Soc.* **2001**, *123*, 183−184.
(4) Colvin, V. L.; Schlamp, M. C.; Alivisatos, A. P. *Nature* **1994**, *370*, 354−357.

DOI: 10.1021/acs.nanolett.6b04816
Nano Lett. XXXX, XXX, XXX−XXX

(5) Tessler, N.; Medvedev, V.; Kaxes, M.; Kan, S.; Banin, U. *Science* **2002**, *295*, 1506−1508.
(6) Kamat, P. V. *J. Phys. Chem. C* **2008**, *112*, 18737−18753.
(7) Kramer, I. J.; Sargent, E. H. *ACS Nano* **2011**, *5*, 8506−8514.
(8) Mora-Seró, I.; Bisquert, J. *J. Phys. Chem. Lett.* **2010**, *1*, 3046−3052.
(9) Kamat, P. V. *Acc. Chem. Res.* **2012**, *45*, 1906−1915.
(10) Zrazhevskiy, P.; Sena, M.; Gao, X. *Chem. Soc. Rev.* **2010**, *39*, 4326−4354.
(11) Deka, S.; Quarta, A.; Lupo, M. G.; Falqui, A.; Boninelli, S.; Giannini, C.; Morello, G.; De Giorgi, M.; Lanzani, G.; Spinella, C.; Cingolani, R.; Pellegrino, T.; Manna, L. *J. Am. Chem. Soc.* **2009**, *131*, 2948−2958.
(12) Park, Y.-S.; Bae, W. K.; Padilha, L. a.; Pietryga, J. M.; Klimov, V. I. *Nano Lett.* **2014**, *14*, 396−402.
(13) Ding, T. X.; Olshansky, J. H.; Leone, S. R.; Alivisatos, A. P. *J. Am. Chem. Soc.* **2015**, *137*, 2021−2029.
(14) Zhu, H.; Song, N.; Lian, T. *J. Am. Chem. Soc.* **2010**, *132*, 15038−15045.
(15) Minotto, A.; Todescato, F.; Fortunati, I.; Signorini, R.; Jasieniak, J. J.; Bozio, R. *J. Phys. Chem. C* **2014**, *118*, 24117−24126.
(16) Bae, W. K.; Padilha, L. a.; Park, Y. S.; McDaniel, H.; Robel, I.; Pietryga, J. M.; Klimov, V. I. *ACS Nano* **2013**, *7*, 3411−3419.
(17) Christodoulou, S.; Rajadell, F.; Casu, A.; Vaccaro, G.; Grim, J. Q.; Genovese, A.; Manna, L.; Climente, J. I.; Meinardi, F.; Rainò, G.; Stöferle, T.; Mahrt, R. F.; Planelles, J.; Brovelli, S.; Moreels, I. *Nat. Commun.* **2015**, *6*, 7905.
(18) Urbach, F. *Phys. Rev.* **1953**, *92*, 1324.
(19) Cody, G. D.; Tiedje, T.; Abeles, B.; Brooks, B.; Goldstein, Y. *Phys. Rev. Lett.* **1981**, *47*, 1480−1483.
(20) Labeau, O.; Tamarat, P.; Lounis, B. *Phys. Rev. Lett.* **2003**, *90*, 257404.
(21) Biadala, L.; Siebers, B.; Gomes, R.; Hens, Z.; Yakovlev, D. R.; Bayer, M. *J. Phys. Chem. C* **2014**, *118*, 22309−22316.
(22) Brovelli, S.; Schaller, R. D.; Crooker, S. A.; García-Santamaría, F.; Chen, Y.; Viswanatha, R.; Hollingsworth, J. A.; Htoon, H.; Klimov, V. I. *Nat. Commun.* **2011**, *2*, 280.
(23) de Mello Donegá, C.; Bode, M.; Meijerink, A. *Phys. Rev. B: Condens. Matter Mater. Phys.* **2006**, *74*, 085320.
(24) Efros, A.; Rosen, M.; Kuno, M.; Nirmal, M.; Norris, D.; Bawendi, M. *Phys. Rev. B: Condens. Matter Mater. Phys.* **1996**, *54*, 4843−4856.
(25) Eilers, J.; van Hest, J.; Meijerink, A.; Donega, C. D. M. *J. Phys. Chem. C* **2014**, *118*, 23313−23319.
(26) Oron, D.; Aharoni, A.; De Mello Donega, C.; van Rijssel, J.; Meijerink, A.; Banin, U. *Phys. Rev. Lett.* **2009**, *102*, 177402.
(27) Rainó, G.; Moreels, I.; Hassinen, A.; Stöferle, T.; Hens, Z.; Mahrt, R. F. *Nano Lett.* **2012**, *12*, 5224−5229.
(28) Wijnen, F. J. P.; Blokland, J. H.; Chin, P. T. K.; Christianen, P. C. M.; Maan, J. C. *Phys. Rev. B: Condens. Matter Mater. Phys.* **2008**, *78*, 235318.
(29) Kamisaka, H.; Kilina, S. V.; Yamashita, K.; Prezhdo, O. V. *J. Phys. Chem. C* **2008**, *112*, 7800−7808.
(30) Jones, M.; Lo, S. S.; Scholes, G. D. *Proc. Natl. Acad. Sci. U. S. A.* **2009**, *106*, 3011−3016.
(31) Voznyy, O.; Thon, S. M.; Ip, A. H.; Sargent, E. H. *J. Phys. Chem. Lett.* **2013**, *4*, 987−992.
(32) Valerini, D.; Cretí, A.; Lomascolo, M.; Manna, L.; Cingolani, R.; Anni, M. *Phys. Rev. B: Condens. Matter Mater. Phys.* **2005**, *71*, 235409.
(33) Eshet, H.; Grünwald, M.; Rabani, E. *Nano Lett.* **2013**, *13*, 5880−5885.
(34) Rainò, G.; Stöferle, T.; Moreels, I.; Gomes, R.; Kamal, J. S.; Hens, Z.; Mahrt, R. F. *ACS Nano* **2011**, *5*, 4031−4036.
(35) Javaux, C.; Mahler, B.; Dubertret, B.; Shabaev, A.; Rodina, A. V.; Efros, A. L.; Yakovlev, D. R.; Liu, F.; Bayer, M.; Camps, G.; Biadala, L.; Buil, S.; Quelin, X.; Hermier, J.-P. *Nat. Nanotechnol.* **2013**, *8*, 206−12.
(36) Shabaev, A.; Rodina, A. V.; Efros, A. L. *Phys. Rev. B: Condens. Matter Mater. Phys.* **2012**, *86*, 205311.
(37) Lupo, M. G.; Della Sala, F.; Carbone, L.; Zavelani-Rossi, M.; Fiore, A.; Lüer, L.; Polli, D.; Cingolani, R.; Manna, L.; Lanzani, G. *Nano Lett.* **2008**, *8*, 4582−4587.
(38) Steiner, D.; Dorfs, D.; Banin, U.; Della Sala, F.; Manna, L.; Millo, O. *Nano Lett.* **2008**, *8*, 2954−2958.
(39) Chilla, G.; Kipp, T.; Menke, T.; Heitmann, D.; Nikolic, M.; Frömsdorf, A.; Kornowski, A.; Förster, S.; Weller, H. *Phys. Rev. Lett.* **2008**, *100*, 057403.
(40) Mittleman, D. M.; Schoenlein, R. W.; Shiang, J. J.; Colvin, V. L.; Alivisatos, A. P.; Shank, C. V. *Phys. Rev. B: Condens. Matter Mater. Phys.* **1994**, *49*, 14435−14447.
(41) Feldmann, J.; Peter, G.; Göbel, E. O.; Dawson, P.; Moore, K.; Foxon, C.; Elliott, R. J. *Phys. Rev. Lett.* **1987**, *59*, 2337−2340.
(42) Gurioli, M.; Vinattieri, A.; Colocci, M.; Deparis, C.; Massies, J.; Neu, G.; Bosacchi, A.; Franchi, S. *Phys. Rev. B: Condens. Matter Mater. Phys.* **1991**, *44*, 3115−3124.
(43) Bronstein, N. D.; Yao, Y.; Xu, L.; O'Brien, E.; Powers, A. S.; Ferry, V. E.; Alivisatos, A. P.; Nuzzo, R. G. *ACS Photonics* **2015**, *2*, 1576−1583.
(44) Benkabou, F.; Aourag, H.; Certier, M. *Mater. Chem. Phys.* **2000**, *66*, 10−16.
(45) Wang, L. W.; Zunger, A. *J. Phys. Chem.* **1994**, *98*, 2158.
(46) Zunger, A.; Wang, L. W. *Appl. Surf. Sci.* **1996**, *102*, 350.
(47) Williamson, A. J.; Zunger, A. *Phys. Rev. B: Condens. Matter Mater. Phys.* **2000**, *61*, 1978.
(48) Rabani, E.; Hetényi, B.; Berne, B. J.; Brus, L. E. *J. Chem. Phys.* **1999**, *110*, 5355−5369.
(49) Toledo, S.; Rabani, E. *J. Comput. Phys.* **2002**, *180*, 256−269.

DOI: 10.1021/acs.nanolett.6b04816
Nano Lett. XXXX, XXX, XXX−XXX